Published in final edited form as:
Cell Rep. 2013 December 12; 5(5): . doi:10.1016/j.celrep.2013.10.050.

Exosome secretion is enhanced by invadopodia and drives invasive behavior

Daisuke Hoshino[1], **Kellye C. Kirkbride**[1], **Kaitlin Costello**[1], **Emily S. Clark**[2], **Seema Sinha**[1], **Nathan Grega-Larson**[3], **Matthew J. Tyska**[3], and **Alissa M. Weaver**[1]

[1]Department of Cancer Biology, Vanderbilt University Medical Center, Nashville, TN 37232, U.S.A

[2]Department of Microbiology and Immunology, University of Miami Medical School, Miami, FL, 33101

[3]Department of Cell and Developmental Biology, Vanderbilt University Medical Center, Nashville, TN 37232, U.S.A

Summary

Unconventional secretion of exosome vesicles from multivesicular endosomes (MVE) occurs across a broad set of systems and is reported to be upregulated in cancer where it promotes aggressive behavior. However, regulatory control of exosome secretion is poorly understood. Using cancer cells, we identified specialized invasive actin structures called invadopodia as specific and critical docking and secretion sites for CD63- and Rab27a-positive MVE. Thus, inhibition of invadopodia formation greatly reduced exosome secretion into conditioned media. Functionally, addition of purified exosomes or inhibition of exosome biogenesis or secretion greatly affected multiple invadopodia lifecycle steps, including invadopodia formation, stabilization, and exocytosis of proteinases, indicating a key role for exosome cargoes in promoting invasive activity and providing *in situ* signaling feedback. Exosome secretion also controlled cellular invasion through 3-dimensional matrix. These data identify a synergistic interaction between invadopodia biogenesis and exosome secretion and reveal a fundamental role for exosomes in promoting cancer cell invasiveness.

INTRODUCTION

Exosomes are small extracellular vesicles that carry functional protein and RNA cargoes and influence cell behavior (Thery, 2011). In cancer, exosomes are thought to promote tumor progression and metastasis (Bobrie et al., 2012; Peinado et al., 2012; Yang and Robbins, 2011). While numerous proteomics studies have identified exosome cargoes, little is known about how exosomes are secreted from cells. Recent studies have identified critical docking factors for multivesicular endosomes (MVE), including Rab27a, Rab27b (Ostrowski et al., 2010), Rab35 and TBC1D10A-C (Hsu et al., 2010). Nonetheless, how exosome docking and secretion sites are specified at the plasma membrane is unknown.

Correspondence to: Alissa M. Weaver.

Invadopodia are actin-rich subcellular structures formed by invasive cancer cells that protrude into and degrade extracellular matrix (ECM). Similar structures are used by normal cells to cross tissue barriers and resorb bone (Murphy and Courtneidge, 2011). Recent studies have shown that ECM-degrading proteinases are secreted preferentially at invadopodia (Artym et al., 2006; Clark and Weaver, 2008; Hoshino et al., 2012b; Steffen et al., 2008). Although originally it was assumed that invadopodia proteinases were transported directly from biosynthetic pathways, the late endosomal/lysosomal (LE/Lys) v-SNARE VAMP7 was found to be necessary for transport of the critical metalloproteinase MT1-MMP to invadopodia (Steffen et al., 2008). These findings raised the possibility that cargo destined for invadopodia may be routed to the plasma membrane via a specialized endolysosomal compartment, such as exosome-containing MVE.

RESULTS

MVE Dynamically Interact with Invadopodia

To determine whether MVE localize to invadopodia, we performed electron and light microscopy experiments. For electron microscopy preparations, invasive SCC61 head and neck squamous cell carcinoma (HNSCC) cells, were cultured overnight on Transwell filter inserts coated with crosslinked gelatin to allow invadopodia formation. Examination of thin sections of these preparations revealed clear examples of LE organelles adjacent to invadopodia-like protrusions, including MVE and LE/Lys hybrid organelles that contain MVE (Figure 1A). To substantiate the possibility that MVE localize to invadopodia, we also performed light microscopy. For immunofluorescent localizations in fixed cells, SCC61 and SCC25-H1047R invadopodia-forming HNSCC cells (Hoshino et al., 2012a) were cultured on invadopodia substrates consisting of fluorescent fibronectin bound to crosslinked gelatin on top of glass coverslips. Invadopodia are evident as actin-rich puncta that colocalize with dark areas of fluorescent matrix degradation. Visualization of immunostained cells revealed that the MVE and exosome marker CD63 localizes at or adjacent to actin-rich invadopodia at ECM degradation sites (Figure 1B).

To visualize the dynamic relationship between invadopodia and MVE, we performed live imaging of cells expressing the exosomal markers CD63 or Rab27a with the invadopodia actin marker tdTomato-F-tractin (F-tractin) (Branch et al., 2012; Hoshino et al., 2012a). In live confocal movies, GFP-CD63- and GFP-Rab27a-positive tubulovesicular structures dynamically surrounded and contacted F-Tractin-positive invadopodia puncta (Figures 1C and 1D and Movie S1). The dynamic interaction between exosome markers and invadopodia was also observed in TIRF movies of the basal plasma membrane (Figures 1E and 1F, Movie S2). We also frequently observed strong nontransient colocalization of exosome markers with invadopodia puncta in the TIRF field (~50% of cells, Figures 1G and 1H and Movie S3). Quantitation of the dynamic interactions from confocal movies revealed that the vast majority of invadopodia interact with CD63-positive vesicles and tubules (Figure 1I), suggesting that invadopodia serve as specific docking sites for MVE. Both the dynamic and stable interactions were reduced in cells expressing specific shRNAs targeting the exosome docking factor Rab27a (Figures 1I and 1J).

Exosome Secretion Controls Invadopodia Biogenesis and Activity

The defining feature of invadopodia is that they mediate ECM degradation. MT1-MMP and other matrix-degrading proteinases have been identified on both exosomes and shed microvesicles (Hakulinen et al., 2008; Muralidharan-Chari et al., 2009); however, it is unknown whether their secretion in those forms relates to invadopodia. To determine if invadopodia proteinases are associated with exosomes in our system, we isolated exosomes from the conditioned media of SCC61 and SCC25-H1047R cells by differential

centrifugation. These cells secrete negligible amounts of microvesicles and abundant exosomes, as validated by electron microscopy and Western blot analysis of exosome pellets (Figures 2A, 2B, and S1C and S1D). Along with the canonical exosome markers CD63 and TSG101, we found that our exosome preparations were positive for the critical invadopodia proteinase MT1-MMP along with other plasma membrane markers, including transferrin receptor (TfR) and EGFR (Figures 2A and S1C). SCC61 exosomes also carried MMP2 (Figure S1C), which we previously localized to invadopodia in those cells (Clark and Weaver, 2008). As expected, the negative control Golgi marker GM130 was not present in exosome preparations (Figures 2A and S1C).

To determine whether exosome secretion affects invadopodia biogenesis or activity, we tested the effect of Rab27a knockdown (KD) in SCC61 and SCC25-H1047R HNSCC cells (Fig S1A). As hypothesized, Rab27a-KD greatly decreased both exosome secretion (Figures 2C and S1E, quantitated by NanoSight nanoparticle tracking analysis) and invadopodia-associated matrix degradation (Figures 2D and 2E; S1F, and S1G). There was also a decrease in the number of invadopodia per cell, defined by colocalization of actin puncta with ECM degradation (Figures 2F and S2H). We also knocked down Synaptotagmin-7 (Syt7) (Fig S1B), which controls fusion of lysosomes with the plasma membrane and likewise found a decrease in exosome secretion and invadopodia numbers and activity (Figures 2E and 2F; and S1E–H). For unclear reasons, there was a greater impact of Syt7-KD on invadopodia activity than on exosome secretion in SCC25-H1047R cells, although the effect was similar in SCC61 cells.

Invadopodia form and mature in stages including assembly, proteinase recruitment, ECM degradation, and disassembly (Artym et al., 2006; Murphy and Courtneidge, 2011). To determine how exosome secretion controls the invadopodia lifecycle, we performed live imaging of control and Rab27a-KD cells expressing the invadopodia marker F-Tractin. We found that loss of Rab27a led to a decrease in both the rate of invadopodia formation, defined as the number of new F-Tractin-positive invadopodia puncta that formed over time, and in the lifetime of invadopodia that did form (Figures 2G–I). To verify that exosomes can induce invadopodia formation, purified exosomes were added to control cells and live imaging was performed. Interestingly, in the first hour after exosome treatment, there was no noticeable increase in invadopodia formation. By contrast, treatment with soluble EGF rapidly induces invadopodia formation (Hoshino et al., 2012a). However, one hour after exosome treatment there was a noticeable increase in the number of new invadopodia formed (Figure 2J, Movie S4). This increase in invadopodia formation occurred regardless of whether growth factors and serum were present in the media. Furthermore, exogenous exosomes also extended invadopodia lifetimes (Figure 2K). These activities were not contained in the microvesicle fraction (Figures S1I and S1J).

To test whether exosomes can also promote invadopodia maturation, as defined by acquisition of extracellular proteinases, we performed live imaging of cells expressing F-Tractin together with the invadopodia proteinase MT1-MMP fused to the superecliptic GFP, pHLuorin. Due to the pH sensitivity of pHLuorin, extracellular MT1-MMP-pHLuorin exhibits greatly enhanced fluorescence and is easily visualized at invadopodia (Branch et al., 2012; Hoshino et al., 2012b). Using this tool, we found that the percent of invadopodia that were MT1-MMP-positive was greatly diminished in Rab27a-KD cells compared to control (Figures 2L and 2M). Thus, a major effect of exosome secretion is to facilitate exocytosis of the key matrix-degrading proteinase MT1-MMP at invadopodia.

Formation of exosomes occurs by intraluminal vesiculation in early endosomes (Hanson and Cashikar, 2012). Two mechanisms of exosome formation have been described, regulated respectively by the endosomal sorting complex required for transport (ESCRT) machinery

(Hanson and Cashikar, 2012) and by ceramide synthesis (Trajkovic et al., 2008). To determine the role of exosome biogenesis pathways in invadopodia activity, we inhibited each pathway. To inhibit ESCRT-mediated exosome biogenesis, we knocked down Hrs, a member of the ESCRT-0 complex (Tamai et al., 2010) (Figure S2A). As expected, Hrs-KD cells secreted significantly fewer exosomes per cell (Figures 3A and S2B). Similar to Rab27a- and Syt7-KD, KD of Hrs also led to large decreases in invadopodia-associated matrix degradation and in the number of invadopodia per cell (Figures 3B–D; S2C–E). We also inhibited ceramide synthesis with the neutral sphingomyelinase-targeting drug GW4869. Consistent with previous findings (Trajkovic et al., 2008), inhibition of ceramide synthesis led to a large decrease in exosome secretion (Figures 3A and S2B). When tested in invadopodia assays, there was a similarly large decrease in invadopodia activity and numbers (Figures 3B–D; S2C–E). These data provide further evidence that exosomes themselves critically control invadopodia biogenesis and function. Furthermore, both the ESCRT and ceramide pathways contribute to invadopodia function.

Because ESCRT and ceramide pathways are thought to generate exosomes with different cargos (Trajkovic et al., 2008), we analyzed exosomes purified from control and Hrs-KD or GW4869-treated cells for the presence of MT1-MMP or the ESCRT protein TSG101. Surprisingly, we found no difference in the cargo content of the exosomes that were generated. When comparing exosomes collected from an equal number of cells, Hrs-KD and GW4869 treatment led to a similar decrease in MT1-MMP- and TSG101-positivity of exosomes and there was no further decrease by combining the two treatments (Figures 3E and 3F). Likewise, when equal numbers of exosomes were loaded onto Western blots, there was no discernable difference in the MT1-MMP or TSG101 content of exosomes isolated from control, Hrs-KD, GW4869-treated or dual-inhibited cells (Figures 3E and 3F). Finally, the combination of Hrs-KD and GW4869 had no greater effect on exosome secretion than either treatment alone (Figure 3A) suggesting that in our cells ESCRT and ceramide synthesis function in the same pathway.

Invadopodia are key secretion sites for exosomes

Aggressive cancer cells are known to secrete large numbers of exosomes (Yang and Robbins, 2011). Our findings that invadopodia are MVE docking sites suggest that the ability of cells to form invadopodia could be a determining factor in the release of exosomes into the extracellular environment. To test this hypothesis, we inhibited two canonical regulators of invadopodia formation: N-WASp and Tks5 (Murphy and Courtneidge, 2011). N-WASp is critical for actin polymerization at invadopodia sites whereas Tks5 serves as a signaling scaffold protein (Murphy and Courtneidge, 2011). N-WASp was inhibited with the specific drug Wiskostatin whereas Tks5 protein abundance was diminished with shRNA (Figure S3A). As expected, inhibition of N-WASp or Tks5 led to decreased invadopodia numbers and activity (Figures 4A and 4B; S3B–D). Consistent with our hypothesis, we found a respective 70% and 80% decrease in the number of exosomes secreted per cell in N-WASp- and Tks5-inhibited cells compared with controls (Figure 4C; similar decreases shown in Figure S3E). Although we cannot rule out invadopodia-independent roles of Tks5 and N-WASp, these data strongly suggest that invadopodia contribute significantly to exosome secretion.

To further test the role of invadopodia in exosome secretion, we determined whether induction of invadopodia could enhance exosome secretion. We and others recently reported that activation of phosphatidylinositol 3-kinase (PI3K) greatly enhances invadopodia formation by cancer cells (Hoshino et al., 2012a; Yamaguchi et al., 2011). We therefore utilized SCC25 HNSCC cells stably engineered to express either an empty vector (SCC25-Control) or the active H1047R mutant of the catalytic subunit of PI3K (SCC25-H1047R). We previously showed that expression of H1047R in SCC25 cells induces invadopodia

formation (Hoshino et al., 2012a), and this cell line was used as a model throughout this manuscript along with the HNSCC cell line SCC61. Quantitation of the concentration of exosomes secreted from an equal number of cells into conditioned media revealed a 6.5-fold increase in exosome release from SCC25-H1047R-expressing cells compared to control SCC25 cells (Figure 4D). These data indicate that invadopodia are key docking sites for MVE and control exosome secretion.

Exosomes Mediate 3D Proteolytic Invasion

In tissues, invadopodia are thought to take the form of 3-dimensional (3D) invasive protrusions and mediate proteolysis-dependent invasion (Gligorijevic et al., 2012; Yu et al., 2012). To determine whether exosome markers were present at actin-rich invasive protrusions in 3D cultures, we performed confocal live imaging of F-Tractin-, GFP-CD63-expressing MDA-MB-231 breast cancer cells embedded in Matrigel. MDA-MB-231 cells were chosen because they form numerous and long protrusions in 3D culture that are ideal for imaging (Yu et al., 2012). Indeed, we found that MDA-MB-231 cells elaborated long protrusions containing both actin and the exosome marker CD63 (Figure 4E). Culturing cells in DQ-collagen IV/Matrigel mixtures to observe matrix degradation revealed DQ-collagen cleavage in association with CD63/actin-positive protrusions (Figure S4C). To determine whether exosome secretion would affect 3D proteolytic invasion, we performed an inverted Matrigel invasion assay (Yu et al., 2012). Invasion in this assay depends on ECM degrading proteases, as demonstrated by inhibition with the broad-spectrum proteinase inhibitor GM6001 (Figures 4F and S4B). Using this assay, we find that invasive migration indeed depends on the exosome docking factor Rab27a (Ostrowski et al., 2010) (Figures 4F and S4). In addition, similar to our results with HNSCC cells, KD of Rab27a and Hrs greatly reduces invadopodia activity in MDA-MB-231 cells (Figure 4G).

DISCUSSION

In summary, we have demonstrated that MVE dynamically associate with invadopodia and invadopodia-like 3D protrusions. Furthermore, exosome secretion is critical for invadopodia formation and function. Invadopodia maturation and ECM degradation are likely dependent on the delivery of MT1-MMP and potentially other proteinases via exosomes. However, we also found that purified exosomes can induce invadopodia formation. Thus, our data identify a major positive feedback loop in which secretion of exosomes at invadopodia may provide further stimulation to either induce *de novo* formation or stabilization of invadopodia.

Induction of invadopodia formation may be a consequence of cell stimulation by the presence of growth factors and/or signaling molecules known to be present on exosomes (Mathivanan et al., 2010). However, it is also possible that exosomal delivery of proteinases, membranes, or additional cargo may contribute to the biogenesis process by stabilizing small nascent invadopodia (see model in Figure S4D). This latter possibility is supported by our finding that exosomes induce invadopodia formation even in the presence of growth factors and serum (Figure 2J). Given the concentration of proteinase and signaling cargoes in exosomes (Thery, 2011), our data provide an appealing mechanism for poorly understood positive feedback loops that are known to control invadopodia (Branch et al., 2012; Murphy and Courtneidge, 2011; Steffen et al., 2008).

Consistent with invadopodia being critical docking sites for exosomes, we found that the presence of invadopodia was a determining factor for exosome secretion. Thus, inhibition or induction of invadopodia formation respectively decreased or increased the concentration of exosomes released into the medium. Although we cannot rule out the existence of other cellular docking sites for exosomes, our data indicate that the molecular makeup of invadopodia greatly facilitates MVE docking and/or secretion.

A critical future direction will be to identify direct molecular interactions between invadopodia molecules and MVE docking factors. A likely candidate is membrane-bound invadopodia signaling molecules like phosphoinositides that could link Rab27a-binding factors to the plasma membrane (Galvez-Santisteban et al., 2012). In addition, adhesion-associated molecules are known to be critical for vesicle capture at invadopodia (Branch et al., 2012) and are good candidates to link to MVE docking factors. It also seems likely that polarized delivery of MVE to invadopodia is an important component of the secretion process. Our findings are reminiscent of a recent study showing that exosome secretion by T-cells takes place at the immune synapse (Mittelbrunn et al., 2011). Given molecular similarities between invadopodia and the immune synapse, including dependence on branched actin, microtubules, integrins, and nonreceptor tyrosine kinase signaling, it seems likely that there is a fundamental molecular combination that specifies targeting and docking sites for MVE. In cancer, enhanced signaling leading to invadopodia formation may thus lead to upregulation of exosome targeting sites with consequent increased secretion, matrix degradation, and overall aggressive behavior.

METHODS

Detailed procedures and reagent information are in the Supplemental Experimental Procedures. SPSS PASW Statistics 18 and GraphPad software packages were used for statistical analyses. Data were analyzed for normality using the Kolmogorov-Smirnov test. Non-parametric data (invadopodia data) were analyzed with Kruskal-Wallis one-way ANOVA, followed by a Tamhane post-hoc test and are represented by medians and box and whiskers plots. Data with a normal distribution (exosomes, Western blot data) were analyzed either using a one-way ANOVA followed by a Bonferroni post hoc test or a student's t-Test and are represented by mean+/−standard error.

Supplementary Material

Refer to Web version on PubMed Central for supplementary material.

Acknowledgments

Funding was provided by NIH grants R01 CA163592 (AMW), R56 DK095811 and R01 DK075555 (MJT), AI060729 and 2R32 MH018917-21 (EC), CTSA grants UL1 RR024975 and TR000445-06, NCI Cancer Center Support Grant P30 CA068485, VUMC CISR grants CA68485, DK20593, DK58404, HD15052, DK59637 and EY08126, American Cancer Society RSG-09-170-01-CSM (AMW), and American Heart Association fellowship 10PRE4030003 (SS).

References

Artym VV, Zhang Y, Seillier-Moiseiwitsch F, Yamada KM, Mueller SC. Dynamic interactions of cortactin and membrane type 1 matrix metalloproteinase at invadopodia: defining the stages of invadopodia formation and function. Cancer Res. 2006; 66:3034–3043. [PubMed: 16540652]

Bobrie A, Krumeich S, Reyal F, Recchi C, Moita LF, Seabra MC, Ostrowski M, Thery C. Rab27a supports exosome-dependent and -independent mechanisms that modify the tumor microenvironment and can promote tumor progression. Cancer Res. 2012; 72:4920–4930. [PubMed: 22865453]

Branch KM, Hoshino D, Weaver AM. Adhesion rings surround invadopodia and promote maturation. Biology Open. 2012; 1:711–722. [PubMed: 23213464]

Clark ES, Weaver AM. A new role for cortactin in invadopodia: Regulation of protease secretion. Eur J Cell Biol. 2008

Galvez-Santisteban M, Rodriguez-Fraticelli AE, Bryant DM, Vergarajauregui S, Yasuda T, Banon-Rodriguez I, Bernascone I, Datta A, Spivak N, Young K, et al. Synaptotagmin-like proteins control

the formation of a single apical membrane domain in epithelial cells. Nat Cell Biol. 2012; 14:838–849. [PubMed: 22820376]

Gligorijevic B, Wyckoff J, Yamaguchi H, Wang Y, Roussos ET, Condeelis J. N-WASP-mediated invadopodium formation is involved in intravasation and lung metastasis of mammary tumors. J Cell Sci. 2012; 125:724–734. [PubMed: 22389406]

Hakulinen J, Sankkila L, Sugiyama N, Lehti K, Keski-Oja J. Secretion of active membrane type 1 matrix metalloproteinase (MMP-14) into extracellular space in microvesicular exosomes. J Cell Biochem. 2008; 105:1211–1218. [PubMed: 18802920]

Hanson PI, Cashikar A. Multivesicular body morphogenesis. Annu Rev Cell Dev Biol. 2012; 28:337–362. [PubMed: 22831642]

Hoshino D, Jourquin J, Emmons SW, Miller T, Goldgof M, Costello K, Tyson DR, Brown B, Lu Y, Prasad NK, et al. Network analysis of the focal adhesion to invadopodia transition identifies a PI3K-PKCalpha invasive signaling axis. Sci Signal. 2012a; 5:ra66. [PubMed: 22969158]

Hoshino D, Koshikawa N, Suzuki T, Quaranta V, Weaver AM, Seiki M, Ichikawa K. Establishment and validation of computational model for MT1-MMP dependent ECM degradation and intervention strategies. PLoS Comput Biol. 2012b; 8:e1002479. [PubMed: 22511862]

Hsu C, Morohashi Y, Yoshimura S, Manrique-Hoyos N, Jung S, Lauterbach MA, Bakhti M, Gronborg M, Mobius W, Rhee J, et al. Regulation of exosome secretion by Rab35 and its GTPase-activating proteins TBC1D10A-C. J Cell Biol. 2010; 189:223–232. [PubMed: 20404108]

Mathivanan S, Ji H, Simpson RJ. Exosomes: extracellular organelles important in intercellular communication. J Proteomics. 2010; 73:1907–1920. [PubMed: 20601276]

Mittelbrunn M, Gutierrez-Vazquez C, Villarroya-Beltri C, Gonzalez S, Sanchez-Cabo F, Gonzalez MA, Bernad A, Sanchez-Madrid F. Unidirectional transfer of microRNA-loaded exosomes from T cells to antigen-presenting cells. Nature communications. 2011; 2:282.

Muralidharan-Chari V, Clancy J, Plou C, Romao M, Chavrier P, Raposo G, D'SouzaSchorey C. ARF6-regulated shedding of tumor cell-derived plasma membrane microvesicles. Curr Biol. 2009; 19:1875–1885. [PubMed: 19896381]

Murphy DA, Courtneidge SA. The 'ins' and 'outs' of podosomes and invadopodia: characteristics, formation and function. Nat Rev Mol Cell Biol. 2011; 12:413–426. [PubMed: 21697900]

Ostrowski M, Carmo NB, Krumeich S, Fanget I, Raposo G, Savina A, Moita CF, Schauer K, Hume AN, Freitas RP, et al. Rab27a and Rab27b control different steps of the exosome secretion pathway. Nat Cell Biol. 2010; 12:19–30. sup pp 11–13. [PubMed: 19966785]

Peinado H, Aleckovic M, Lavotshkin S, Matei I, Costa-Silva B, Moreno-Bueno G, Hergueta-Redondo M, Williams C, Garcia-Santos G, Ghajar C, et al. Melanoma exosomes educate bone marrow progenitor cells toward a pro-metastatic phenotype through MET. Nat Med. 2012; 18:883–891. [PubMed: 22635005]

Steffen A, Le Dez G, Poincloux R, Recchi C, Nassoy P, Rottner K, Galli T, Chavrier P. MT1-MMP-dependent invasion is regulated by TI-VAMP/VAMP7. Curr Biol. 2008; 18:926–931. [PubMed: 18571410]

Tamai K, Tanaka N, Nakano T, Kakazu E, Kondo Y, Inoue J, Shiina M, Fukushima K, Hoshino T, Sano K, et al. Exosome secretion of dendritic cells is regulated by Hrs, an ESCRT-0 protein. Biochem Biophys Res Commun. 2010; 399:384–390. [PubMed: 20673754]

Thery C. Exosomes: secreted vesicles and intercellular communications. F1000 biology reports. 2011; 3:15. [PubMed: 21876726]

Trajkovic K, Hsu C, Chiantia S, Rajendran L, Wenzel D, Wieland F, Schwille P, Brugger B, Simons M. Ceramide triggers budding of exosome vesicles into multivesicular endosomes. Science. 2008; 319:1244–1247. [PubMed: 18309083]

Yamaguchi H, Yoshida S, Muroi E, Yoshida N, Kawamura M, Kouchi Z, Nakamura Y, Sakai R, Fukami K. Phosphoinositide 3-kinase signaling pathway mediated by p110alpha regulates invadopodia formation. J Cell Biol. 2011; 193:1275–1288. [PubMed: 21708979]

Yang C, Robbins PD. The roles of tumor-derived exosomes in cancer pathogenesis. Clinical & developmental immunology. 2011; 2011:842849. [PubMed: 22190973]

Yu X, Zech T, McDonald L, Gonzalez EG, Li A, Macpherson I, Schwarz JP, Spence H, Futo K, Timpson P, et al. N-WASP coordinates the delivery and F-actin-mediated capture of MT1-MMP at invasive pseudopods. J Cell Biol. 2012; 199:527–544. [PubMed: 23091069]

Highlights

- Invadopodia are key docking sites for exosome-containing multivesicular endosomes
- Invadopodia regulators control the quantity of exosomes secreted from cancer cells
- Exosome secretion controls invadopodia biogenesis and matrix-degrading activity
- A synergistic relationship exists between exosomes and invadopodia

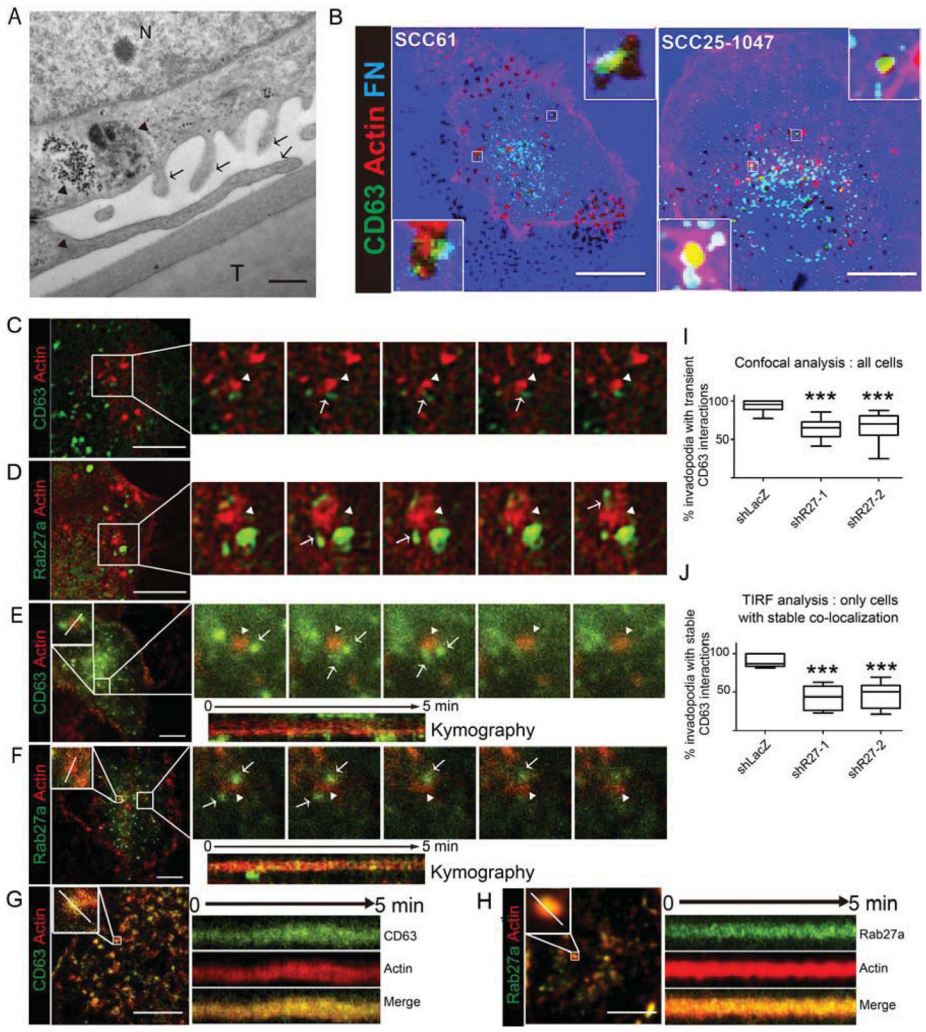

Figure 1. MVE are recruited to invadopodia sites

(A) SCC61 cells cultured on crosslinked gelatin-coated Transwell filters. Arrows point to invadopodia. Arrowheads point to MVE and MVE-containing autophagolysosomes docked near invadopodia. N = nucleus. T = Transwell filter. (B) Confocal images of cells expressing GFP-CD63 (green) cultured on Alexa-633-fibronectin (FN)-coated gelatin (blue) and stained with rhodamine phalloidin (red) to detect actin filaments. Dark spots in the FN images indicate degradation. Scale bars=10 μm. (C–F) SCC25-H1047R cells stably expressing F-tractin (red) were transfected with GFP-CD63 (C,E) or GFP-Rab27a (D,F) (green) and cultured for 24 h on FN-coated gelatin plates for live confocal microscopy (C,D) or on FN-coated plates for live TIRF microscopy (E–H). Frame rates are 1 per 0.97 sec (confocal) or 1 per 2.8 sec (TIRF). Sequential frames show transient and tubular interactions of green GFP-CD63- or GFP-Rab27a-positive vesicular structures (arrows) with invadopodia (arrowheads). Scale bars=20 μm (C,D) or 10 μm (E,F,G,H). (G,H): TIRF movies showing stable colocalization of GFP-CD63 and GFP-Rab27a with invadopodia. Kymographs show examples of transient (E,F) and stable (G,H) interactions between exosome markers and invadopodia. (I,J) Percent invadopodia per cell with transient (I) or stable (J) interactions with GFP-CD63-positive endosomes in control (shLacZ) and Rab27a-KD (shR27) cells. Data plotted as box-and-whiskers plots where the median is represented with a line, the box

represents the 25–75 percentile, and error bars show the 5–95 percentile. ***$p<0.001$. $N \geq 10$ cells from 10 movies from ≥3 independent experiments.

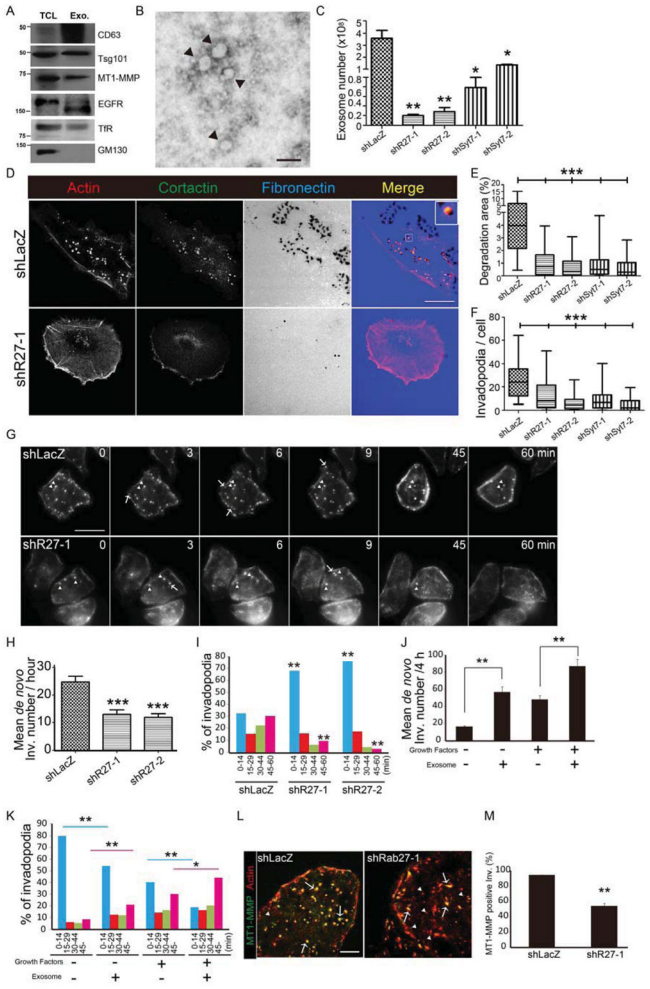

Figure 2. Exosome secretion promotes invadopodia formation and maturation

(A) Western blot analysis of proteins in SCC25-H1047R total cell lysates (TCL) and exosomes (Exo.). (B) Negatively stained EM image of purified exosomes (indicated by arrowheads). Scale bar=100 nm. (C) NanoSight quantification of exosome numbers purified from cell culture supernatants from 3 independent experiments. Mean+/−SEM. (D) Images of SCC25-H1047R control (shLacZ) and Rab27a KD cells (shR27-1) cultured on FN (blue) coated gelatin plates and immunostained for cortactin (green) and F-actin (red). Scale bars=20 μm. n > 53 cells per cell line from 3 independent experiments. (E) Quantification of invadopodia mediated ECM degradation (% cell area). (F) Quantification of invadopodia number per cell. Data plotted as box-and-whiskers plots. (G) shLacZ and shR27-1 cells expressing F-tractin were plated on FN-coated gelatin plates for live imaging (1 frame per 90 s for 60 min). Arrowheads: stable invadopodia, Arrows: newly formed invadopodia. Scale bar, 20 μm. n>30 cells per cell line from 5 independent experiments. (H) Rate of invadopodia formation from movies. (I) Invadopodia lifetime, quantitated as length of time an invadopodia persists after formation. Asterisks show statistical comparisons to similar time bins in shLacZ control cells. (J,K) SCC25-H1047R shLacZ expressing F-tractin were cultured on FN-coated gelatin plates with or without growth factors before adding 2×10^6 exosomes derived from SCC25-H1047R cells stably expressing GFP-CD63. After 1 h, live movies (Movie S4) were obtained as in (G). (J) Rate of invadopodia formation. (K) Invadopodia lifetime. n>13 cells per condition from 3 independent experiments. Pink and blue lines indicate statistical comparisons between pink and blue bars in graph. (L) TIRF

images of shLacZ and shR27-1 cells stably expressing F-tractin (red, “Actin”) and transfected with MT1-MMP-pHluorin (green, “MT1-MMP”). Arrowheads indicate actin only and arrows show MT1-MMP-positive actin puncta. Scale bar=10 μm. n>10 cells per condition from 3 independent experiments. (M) Quantification of % MT1-MMP-positive invadopodia. * $p<0.05$, **, $p<0.01$, ***$p<0.001$. See also Figure S1.

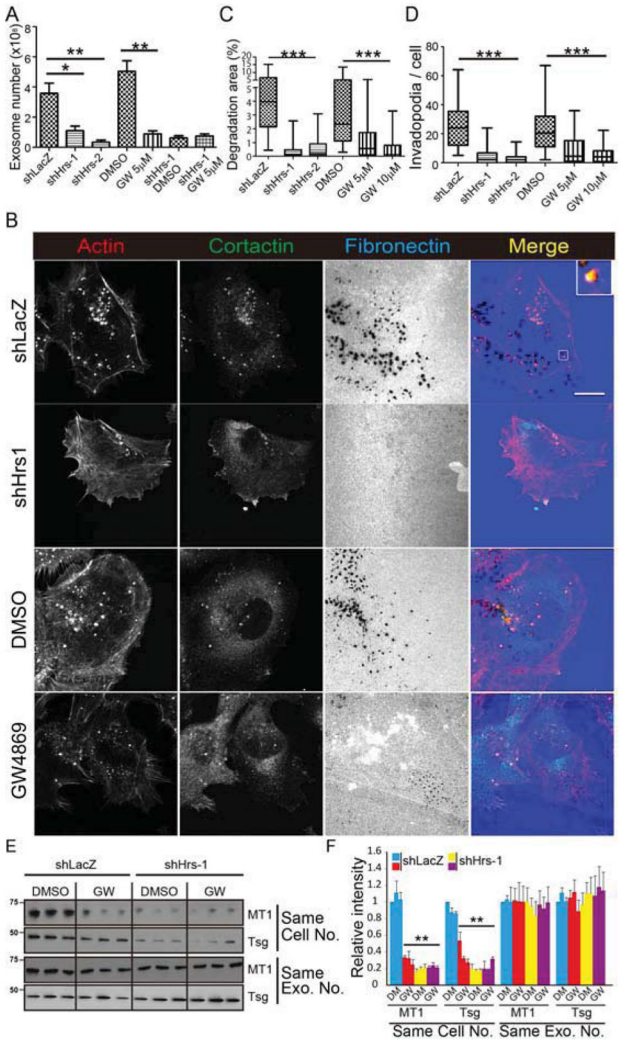

Figure 3. Exosome biogenesis controls invadopodia activity

(A) Quantification of exosome numbers. N=3 independent experiments. (B) Images of SCC25-H1047R control (shLacZ), Hrs knockdown (shHrs-1), DMSO- and GW4869 (GW)-treated cells cultured on invadopodia plates. Scale bars 20=μm. n>51 cells per condition from 3 independent experiments. (C) Invadopodia-associated ECM degradation. (D) Invadopodia number per cell. Data plotted as box-and-whiskers plots. (E) Western blot analysis of exosomes with gel loading based on the same number of cells (upper panels) or with equal exosome numbers (bottom two panels). Cell conditions (control, Hrs-KD, GW treatment or both) as indicated. N=3 independent experiments. (F) Quantification of E, mean +/−SEM. Control shLacZ data for A,C,D are the same as 2C,E,F. * p<0.05, **, p<0.01, ***p<0.001. See also Figure S2.

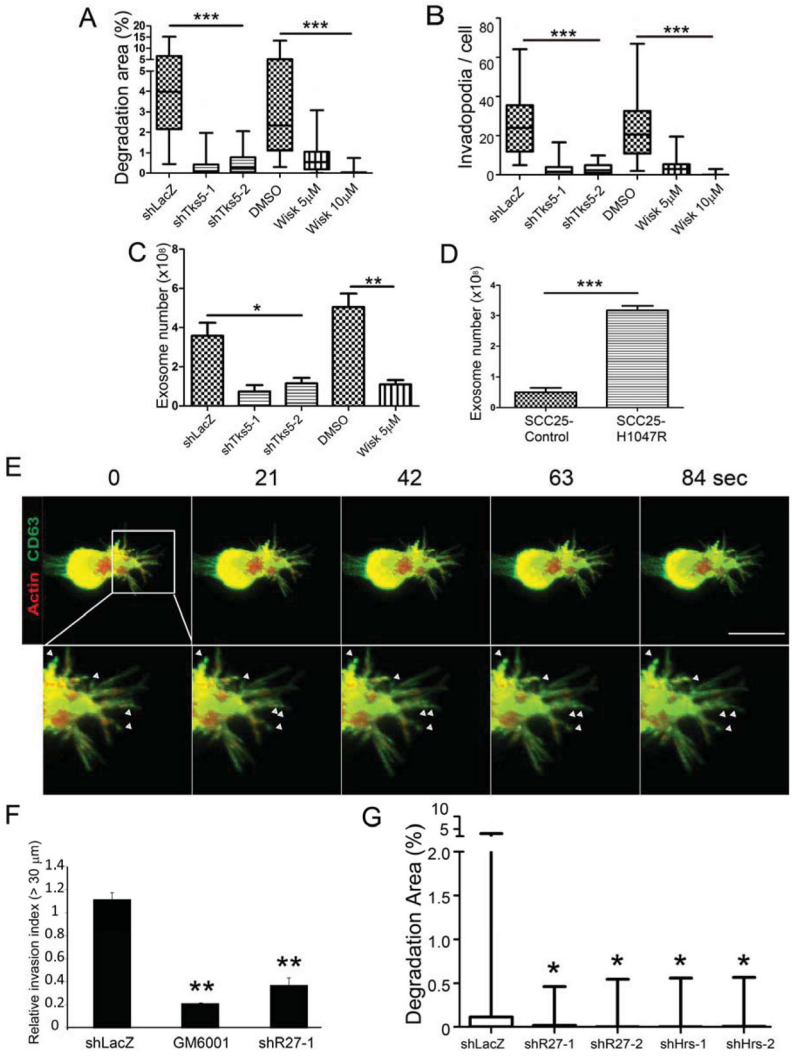

Figure 4. Invadopodia and exosomes have a reciprocal relationship to control exosome secretion and 3D invasion

Invadopodia-associated ECM degradation (A) and invadopodia number per cell (B) in Tks5-KD (shTks5) or Wiskostatin (Wisk)-treated SCC25-H1047R cells compared to shLacZ or DMSO controls. Data plotted as box-and-whiskers plots. n > 54 cells per cell line from 3 independent experiments. (C,D) Exosome numbers under invadopodia inhibition (C, shTks5 or Wisk) or induction (D, H1047R compared to control) conditions. n=3 independent experiments. Mean +/−SEM. (E) MDA-MB-231 cells stably expressing GFP-CD63 were transfected with F-tractin, embedded in matrigel and cultured for 24 h. Arrowheads indicate punctate accumulations of CD63 in protrusions. Frames every 21 s. Scale Bar=10 μm. (F) Inverted invasion assay. Control (shLacZ) or Rab27a-KD (shR27-1) MDA-MB-231 cells migrated into Matrigel plugs for 72 h before staining with Hoechst and confocal imaging. Invasion capacity quantitated as the fluorescence intensity of cells penetrating ≥30 μm, normalized to median shLacZ value. Mean+/−SEM. N=3 independent experiments, with duplicates per condition. (G) Invadopodia-associated ECM degradation by MDA-MB-231 cells. Box-and-whiskers plots. n > 45 cells per cell line from 3 independent experiments. Control shLacZ and DMSO data for A,B,C are the same as 2C,E,F and 3A,C,D, respectively. * p<0.05, **, p<0.01, ***p<0.001. See also Figures S3 and S4.